RESEARCH ARTICLE

BULLETIN OF ECONOMIC RESEARCH

Pandemic effects in the Solow growth model

Julio Carmona | Ángel León

Departamento de Fundamentos del
Análisis Económico, University of
Alicante, Alacant, Spain

Correspondence
Julio Carmona, Departamento de
Fundamentos del Análisis Económico,
University of Alicante, Campus de Sant
Vicent del Raspeig, Alacant, 03080, Spain.
Email: carmona@ua.es

Abstract
We show how diseases can affect economic growth in a Solow growth model, with population growth and no technical progress, but modified to include a saving rate that depends on the individual health status. We successively insert this model into the SIS (susceptible–infected–susceptible) and SIR (susceptible–infected–recovered) models of disease spreading. In these two models, the spread of the infection proceeds according to the so-called basic reproductive number. This number determines in which of the two possible equilibria, the disease-free or the pandemic equilibrium, the economy ends. We show that output per capita is always lower in the pandemic steady state, which implies a contraction in the economy's production possibilities frontier.

KEYWORDS
COVID-19, SIS, SIR, Solow model

JEL CLASSIFICATION
E00, I15, O40

1 | INTRODUCTION

There is no doubt that the outbreak and the subsequent expansion of the COVID-19 pandemic has caused a surge in the interest on its economic consequences. The paper of Avery et al. (2020) provides a relevant example with a summary of the epidemiological literature and suggestions for policy contributions from Economics. Hethcote (2008) provides an excellent summary to the

basic epidemiological models used in the literature. The standard approach is to separate population into several nonoverlapping compartments. So, the total population is typically divided into susceptible of infection individuals, infected individuals, and recovered (or dead) individuals. Given those groups, two basic models have been widely used in the literature: the SIS (susceptible–infected–susceptible) and the SIR (susceptible–infected–recovered) models. In the SIS model, the subgroup of susceptible individuals can become infected after contact with an infected individual. Once they are recovered, they become susceptible again because, due perhaps to mutations in the virus, they do not develop immunity. This is typical of diseases such as influenza, malaria, or measles. However, in the SIR model, the subgroup of recovered individuals is added to include those individuals that develop permanent immunity after recovery from the disease. Thus, they do not return to the category of susceptibles after passing the disease as in the SIS model. This is the standard approach followed to analyze the COVID-19 disease caused by the SARS-Cov 2 virus.

Both models provide basic insights within a tractable framework which is amenable to many straightforward extensions. This is because, despite their simplicity, there are lessons that can be learned from them and some intuitions can be developed about the evolution of pandemics. For instance, dos Santos et al. (2021) use the canonical SIR model with time-varying parameters to account for the evolution of the disease in Brazil and other countries. Roda et al. (2020) show that an SIR model performs better than a more general SEIR (susceptible–exposed–infected–recovered) model[1] to explain the COVID-19 data in Wuhan and other regions of China. Ahmetolan et al. (2020) use this model to estimate robustly the timings of the maximum and the timings of the inflection points of the proportion of infected individuals.[2]

In the conventional approach, both SIS and SIR models assume that total population is constant and fixed. This setup has been considered by some authors to examine the impact of optimal decisions about social distancing and their effect on the spread of the disease. For instance, Fernandez-Villaverde and Jones (2020) estimate an SIR model that includes a fatality rate, that represents an excess of mortality above that level that would be observed without the disease, with time-varying parameters as a result of not modeling agents' endogenous decisions. Eichenbaum et al. (2020) model the interactions between economic decisions and epidemic in an otherwise standard New-Keynesian model. They show that these decisions exacerbate the recession caused by the epidemic. Finally, Acemoglu et al. (2020) develop a multirisk SIR model where infection, hospitalization, and fatality rates vary depending on group age. They show that targeting by age lockdowns outperforms those that cover all the population uniformly and that the use of measures of testing, tracing, and isolation of the infected can minimize economic losses and death costs.

All previous studies focus on the short run with a constant population. However, as Hethcote (2008) points out, a constant population is only a sensible assumption when the disease spreads quickly in the population and dies out within a short period of time. Furthermore, the fixed population assumption can also be reasonable in a medium- to long-term horizon if the birth and the death rates are not too different and the population size is constant or nearly constant.

As the current situation of the disease suggests, it is not at all clear that the COVID-19 is a transient situation that will disappear with vaccination. The lack of cover for poorer countries has caused the appearance of new variants which are even more contagious and lethal. This suggests that the disease may not be a short-run phenomenon and it can be of interest to examine its medium to long-run consequences. For instance, the International Monetary Fund's 2021 April issue of the World Economic Outlook includes forecasts of the potential GDP paths for most

---

[1] The *exposed* group consists of those individuals who are in a latent period of the infection before being infected.

[2] See Moein et al. (2021) for evidence against the ability of the SIR model to forecast COVID-19 epidemic.

developed countries, which do not show any seeming consequences of the disease. However, its persistence might cause that those predictions turned out to be very misleading.

The problem of the long-run economic impact of diseases has been considered in the economic development literature by putting emphasis on the optimal level of health expenditure. For instance, Goenka et al. (2014) introduces a model that joins the standard SIS model with a neoclassical growth model which includes a health production sector. In this setup, they find the optimal health expenditure by a benevolent social planner. Goenka and Liu (2020), based on Gersowitz and Hammer (2004), expand their former model to analyze the decentralized solution to health expenditure, in which households ignore the externality imposed by disease transmission. Recently, Goenka et al. (2021) has developed a model joining the SIR model with the standard one-sector neoclassical growth model. In this case, the disease causes an increase in the mortality rate so that the death rate is higher than otherwise.

Our paper is a simple approximation to the consequences of diseases on the level of per capita output. As Goenka and Liu (2012) point out, there are three channels through which diseases may affect that variable: changes in labor productivity, changes in human capital accumulation, and changes in the growth path of total population. In their paper, only the first channel is explored within a discrete-time setup. This allows them to show a rich set of dynamic paths that depend only upon the parameters governing the disease dynamics. However, our paper explores a simple extension that also affects per capita output. This is related to the fact that the saving rate of healthy and sick individuals need not be the same if there are limitations to complete insurance against the disease. We shall explore the consequences for the steady-state values of the relevant economic variables, namely, the capital stock per nonsick individual and the levels of output and consumption per capita, of an aggregate saving rate that depends upon the proportion of sick individuals in the population.

To have a reference of the main results in the disease literature, we first review the basic SIS and SIR models when there is positive exponential growth. Considering, the fraction of infected and healthy individuals, we can find two possible steady states: the disease-free solution, in which the society arrives to a situation in which nobody is sick and the endemic solution, in which the proportion of infected individuals is nonzero. The economy will arrive to one or another equilibrium depending upon the so-called basic reproductive number, henceforth $\mathcal{R}_0$. For a stationary population, this is defined as the ratio between the rate of infection and the rate of recovery. When the rate of population growth is positive, the denominator of the basic reproductive number must include the population birth rate.[3] In general, the proportion of infected individuals in the SIR model is typically lower than in the SIS model. Furthermore, convergence to the pandemic steady state in the case of the SIR model may be cyclical.

We aim to couple each model of disease with a simple one-sector growth model in which the aggregate saving rate depends upon the fraction of infected individuals. Except for that feature, our representation of the economy agrees with the one-sector growth model with a Cobb–Douglas production function and the stock accumulation equation that can be found in Jones and Vollrath (2013). For each model of disease, we discuss its implications for the steady-state value of the capital stock per worker and hence, for the level of output per capita. Observe that, provided that only healthy people can work, instead of the conventional capital labor ratio we use the ratio between the economy's capital stock and the number of noninfected individuals in the population.

---

[3] This is a standard result in the epidemiological literature. See Hethcote (2008) for an excellent summary. In the context of growth models, Goenka and Liu (2012), Goenka et al. (2014), and Goenka and Liu (2020) also find a disease-free and an endemic steady state depending on $\mathcal{R}_0$.

This implies that the relevant growth rate for the labor force changes during the transition period, from one steady state to another. But once the economy achieves the new steady state with a given long-run proportion of SIR individuals, the rate of change of the labor force equals the rate of growth of the population.

The main result of the paper is that output per capita is always lower in the pandemic steady state. This is true even in the case that a higher propensity to save by nonhealthy individuals makes both, the aggregate saving rate and the capital stock per noninfected individual greater than in the disease-free steady state. In this case, the steady-state value of consumption per capita is also lower but it could be higher when the saving rate of healthy individuals is greater than the corresponding one for sick individuals.

Our paper is organized as follows. In Sections 2 and 3, we summarize the consequences of a positive population growth rate upon the SIS and SIR models, respectively. Then, each model is inserted into a Solow growth model, with a saving rate that changes with the number of infected people, in Sections 4 and 5. The paper concludes with a summary of the results and some suggestions for future extensions in Section 6. The proofs of the main results can be found in the Appendix.

2 | THE SIS MODEL WITH POSITIVE POPULATION GROWTH

In the canonical SIS model, total population, $N(t)$, is divided into two classes, susceptible of infection individuals, $X(t)$, or susceptibles for short, and infected individuals, $Z(t)$, who once recovered they become susceptible again. In this model, individuals are randomly matched according to some probability. Specifically, the flows out of the class of susceptibles and into the class of infectious are given by the so-called *standard incidence*, see Martcheva (2015), defined as:

$$\frac{bX(t)Z(t)}{N(t)}, \tag{1}$$

where b is the rate of infection per unit time. It measures the average number of contacts made by a susceptible individual that ends in contagion. Similarly, the flows out of the class of infectious and into the class of susceptible are given by the rate of recovery from infection per unit time, a.

Next, population growth is assumed to be exponential as in the Solow growth model. Let us denote the population vegetative growth rate as $g = n - \mu$, where n and μ are, respectively, the birth and death rates. By assuming that all newly born are initially part of the population of susceptible individuals, the dynamics of the two classes in the SIS model are described by the following system of differential equations:

$$\dot{X}(t) = -b\frac{X(t)Z(t)}{N(t)} + aZ(t) + nN(t) - \mu X(t), \tag{2}$$

$$\dot{Z}(t) = b\frac{X(t)Z(t)}{N(t)} - aZ(t) - \mu Z(t). \tag{3}$$

For simplicity, the death rate is assumed to be the same for susceptible and infected individuals. Notice that $\dot{X}(t) + \dot{Z}(t) = (n - \mu)N(t) = gN(t)$.

Considering the per capita variables $x(t) = X(t)/N(t)$ and $z(t) = Z(t)/N(t)$, the systems (2) and (3) can be rewritten in per capita terms as

$$\dot{x}(t) = -bx(t)z(t) + az(t) + n(1 - x(t)), \tag{4}$$

$$\dot{z}(t) = (bx(t) - (a + n))z(t). \tag{5}$$

Since $x(t) + z(t) = 1$, it is straightforward to rewrite Equation (5) as a *Bernoulli equation* and then, find an explicit solution. Specifically, by defining $\mathcal{R}_0 = \dfrac{b}{a + n}$, we get the well-known result that if $\mathcal{R}_0 > 1$ then $z(t) \to z^* = 1 - \dfrac{1}{\mathcal{R}_0}$ and $x(t) \to x^* = \dfrac{1}{\mathcal{R}_0}$ as $t \to \infty$. This defines the *endemic* steady state. When $\mathcal{R}_0 \leqq 1$, $z(t)$ approaches 0 and hence $x(t)$ approaches 1 as $t \to \infty$. This defines the *disease-free* steady state which we will denote as $x^{**} = 1$ and $z^{**} = 0$.

Note that $\mathcal{R}_0$ is the so-called basic reproductive number. When there is population growth, its interpretation is as follows.[4] The time that the proportion of infected individual remains in the infected state follows an exponential distribution with parameter $a + n$. Then, the expected time in the infected state is $1/(a + n)$. With b as the infection fraction per unit time of susceptible individuals, each infected person has an expected number of $\mathcal{R}_0$ contacts while infected. Therefore, $\mathcal{R}_0$ can be interpreted as the expected number of transmissions that a newly infected individual can make if everybody else is susceptible. Moreover, its inverse defines the *herd immunity threshold*, precisely the steady-state proportion of susceptible individuals. This is so because, once achieved, any outburst of the disease dies out quickly.

3 | THE SIR MODEL WITH POSITIVE POPULATION GROWTH

Now, we turn to discuss the SIR model, in which the COVID-19 disease is typically analyzed. In this case, total population, $N(t)$, is divided into three classes: susceptible of infection individuals, $X(t)$, infected individuals, $Z(t)$, and recovered individuals, $V(t)$. As in the description of the SIS model, we choose the standard incidence version given in Equation (1).

By assuming that all newly born are initially part of the population of susceptible individuals and that the rate of death is the same for every individual, independently of the class, we have the following system of equations that describe the evolution of the fraction of susceptibles, $x(t) = X(t)/N(t)$, infected, $z(t) = Z(t)/N(t)$, and recovered individuals, $v(t) = V(t)/N(t)$ in the population:[5]

$$\dot{x}(t) = -bx(t)z(t) + n(1 - x(t)), \tag{6}$$

$$\dot{z}(t) = (bx(t) - (a + n))z(t), \tag{7}$$

---

[4] Avery et al. (2020) provide a similar explanation for the case of a constant population, which is analogous to the explanation in Hethcote (2008) for the case $g = 0$.

[5] See Martcheva (2015) for the solution of an SIR model in which population growths according to the logistic model.

$$\dot{v}(t) = az(t) - nv(t). \tag{8}$$

Proposition 1. *Let $\mathcal{R}_0$ be as defined in the previous section. Then, for $\mathcal{R}_0 \leqq 1$, the disease-free steady state for the systems (6), (7) and (8) is given by:*

$$x^{**} = 1, \quad z^{**} = 0, \quad and \quad v^{**} = 0. \tag{9}$$

Whereas, for $\mathcal{R}_0 > 1$, the pandemic solution is given by:

$$x^* = \frac{1}{\mathcal{R}_0}, \quad z^* = \left(\frac{n}{a+n}\right)\left(1 - \frac{1}{\mathcal{R}_0}\right), \quad and \quad v^* = \left(\frac{a}{a+n}\right)\left(1 - \frac{1}{\mathcal{R}_0}\right). \tag{10}$$

Proof. It follows trivially from setting $\dot{x}(t)$, $\dot{z}(t)$, and $\dot{v}(t)$ to zero. ☐

The former system has no closed-form solution and its stability can only be ascertained by linearizing it around the steady-state solution. Since one of the equations is redundant, given that $\dot{x}(t) + \dot{z}(t) + \dot{v}(t) = 0$, we shall focus on the equations for the dynamics of the population of susceptible and infected individuals.

Proposition 2. *The linearized system to (6) and (7) is given by the matrix equation:*

$$\begin{bmatrix} \dot{x} \\ \dot{z} \end{bmatrix} = \begin{bmatrix} -n\mathcal{R}_0 & -(a+n) \\ n(\mathcal{R}_0 - 1) & 0 \end{bmatrix} \begin{bmatrix} x \\ z \end{bmatrix}. \tag{11}$$

Assume that $\mathcal{R}_0 > 1$, the eigenvalues of system (11) are two imaginary roots with negative real part whenever $n\theta_1 < b < n\theta_2$, where $\theta_i = 2(\frac{a+n}{n})^2(1 \pm \sqrt{\frac{a}{1+a}})$. In any other case, the two roots are real and negative. Therefore, the pandemic steady state is always locally stable but its convergence may be cyclical.

Proof. See the Appendix for the proof. ☐

The cyclical convergence to the pandemic solution is illustrated in Figure 1 for parameter values $a = 0.15$, $b = 0.6$, and $n = 0.03$. The green arrows show the motion of the variables. They set a circle around the steady state (x^*, z^*). Given some initial small bursting of the infection, $z_0 = 0.01$, the true path followed by the proportion of susceptible and infected individuals is also shown by the red curve.[6]

As in Section 2 where we discussed the SIS model, the proportion of infected individuals grows until the population achieves *herd immunity* as given by the inverse of the basic reproductive number $\mathcal{R}_0$. Notice that, in the absence of an explicit solution to the system of differential equations, we cannot know the maximum proportion of infected individuals, as in Section 2, because the population develops immunity after recovering from the disease so that we only know that, once population has achieved the herd immunity threshold, the value of the infected plus the recovered population is $z + v = 1 - 1/\mathcal{R}_0$.

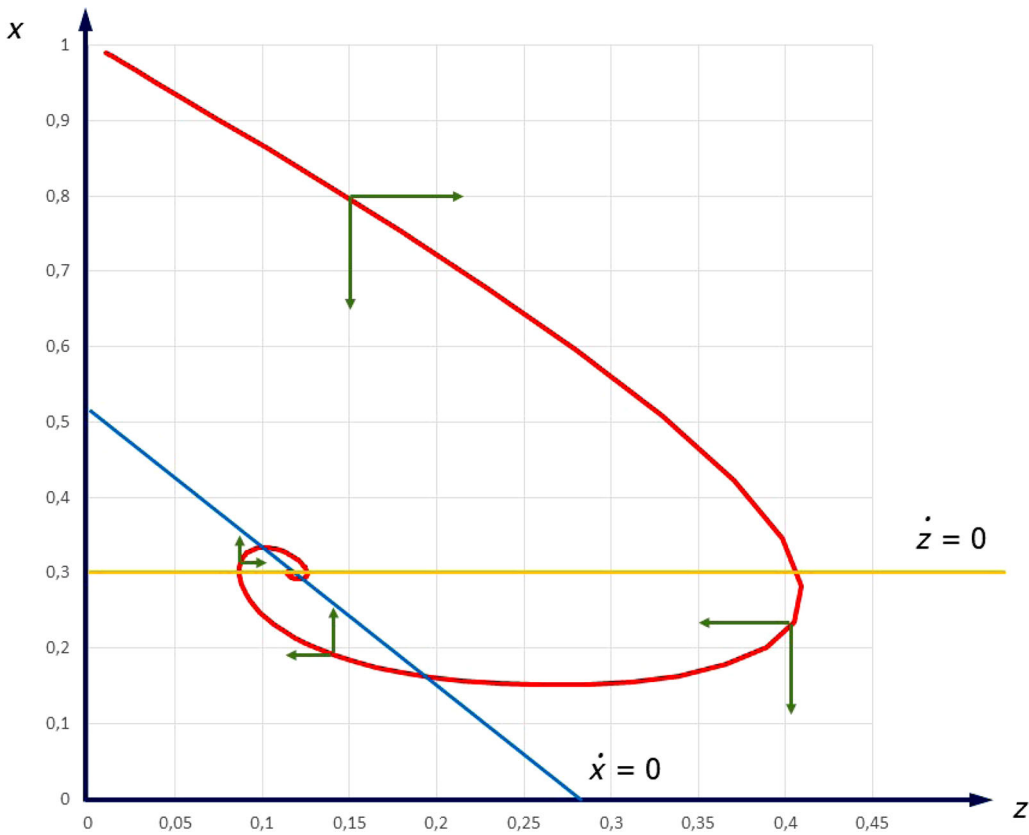[6] This path has been obtained by simulating the differential equations (6) and (7).

FIGURE 1   Linearized SIR model with population growth. The adjustment path (in red) has been obtained using the following set of parameters: $z_0 = 0.01$, $a = 0.15$, $b = 0.6$, and $n = 0.03$. Hence, $x^* = 0.30$ and $z^* = 0.1167$. [Colour figure can be viewed at wileyonlinelibrary.com]

Finally, there is an interesting feature in this version of the SIR model with population growth which is worth to mention. When the population is fixed, $n = 0$, the proportion of infected individuals falls to zero after *herd immunity* is achieved. This is not the case here because the population is growing and there will always be a positive proportion of infected individuals in the long run. Even with a constant population but a positive birth rate (and hence, equal to the death rate) the behavior of $x(t)$ and $z(t)$ might be cyclical until the steady state were eventually reached.

4 | THE SIS PANDEMIC SOLOW MODEL

We now discuss the impact of coupling the SIS model together with the Solow model, henceforth the SIS pandemic Solow model. Let total output be defined by a constant-returns-to-scale production function, $Y(t) = AK(t)^\alpha X(t)^{1-\alpha}$, with parameters A, the total factor productivity index, and α the share of profits in aggregate income. Observe that the only difference with the conventional formulation is that we have substituted the number of susceptible individuals, $X(t)$, for the total

population, $N(t)$. Then, the capital stock accumulation equation is given by

$$\dot{K}(t) = s(z(t))Y(t) - \delta K(t), \tag{12}$$

where δ the capital stock depreciation rate. The term $s(z(t))$ reflects the fact that the aggregate saving rate may depend upon the fraction of infected individuals in the population. Specifically, we assume that the aggregate saving rate is given by

$$s = s_x x(t) + s_z z(t) = s_x - (s_x - s_z)z(t), \tag{13}$$

where s_x is the propensity to save if the individual is susceptible and s_z if the individual is infected.

Since infected individuals cannot work, to obtain the capital stock accumulation equation per effective worker, we must divide both sides by $X(t)$, and not by $N(t)$, then

$$\dot{k}(t) = \frac{\dot{K}(t)}{X(t)} - \frac{\dot{X}(t)}{X(t)}k(t) = [s_x - (s_x - s_z)z(t)]Ak(t)^\alpha - \left(\delta + \frac{\dot{X}(t)}{X(t)}\right)k(t). \tag{14}$$

Since $\dot{x}(t) = \frac{\dot{X}(t)}{N(t)} - gx(t)$, we can write Equation (14) as

$$\dot{k}(t) = [s_x - (s_x - s_z)z(t)]Ak(t)^\alpha - \left(\delta + g + \frac{\dot{x}(t)}{x(t)}\right)k(t), \tag{15}$$

where $\dot{x}(t)$ is given in Equation (4). Summing up, the system of differential equations for the SIS pandemic Solow model that shows the joint dynamics of $x(t)$ and $k(t)$ is driven, respectively, by Equations (4) and (15).

Proposition 3. *If $\mathcal{R}_0 \leqq 1$, the disease-free steady state for the SIS pandemic Solow model is*

$$x^{**} = 1, \quad k^{**} = \left(\frac{s_x A}{\delta + g}\right)^{\frac{1}{(1-\alpha)}}. \tag{16}$$

Alternatively, if $\mathcal{R}_0 > 1$, the pandemic steady state is defined by:

$$x^* = \frac{1}{\mathcal{R}_0}, \quad k^* = \left(\frac{s_x x^* + s_z z^*}{s_x}\right)^{\frac{1}{(1-\alpha)}} k^{**}; \tag{17}$$

so that

$$k^* \gtreqqless k^{**} \quad \Longleftrightarrow \quad s_z \gtreqqless s_x. \tag{18}$$

Proof. The two equilibria follow from setting $\dot{x}(t) = 0$ in Equation (4) and $\dot{k}(t) = 0$ in Equation (15). In the case of the pandemic steady state, the value of the capital stock per noninfected individual is given by $k^{**} = (\frac{[s_x x^* + s_z z^*]A}{\delta + g})^{\frac{1}{(1-\alpha)}}$, which can be rewritten as in (17) simply by multiplying and dividing by s_x. $\qquad\square$

Observe that the steady-state value of the capital stock per noninfected individual does depend upon the relative size of s_x and s_z. The reason is straightforward. Since, z^* is always positive in the pandemic steady state, when $s_x > s_z$, the aggregate saving rate is lower than in the disease-free steady state, so that $k^* < k^{**}$. However, when $s_x < s_z$, the aggregate saving rate is greater than in the disease-free steady state and $k^* > k^{**}$. If full insurance were feasible, both saving rates would be equal and hence, there would be no effect upon the steady-state value of k. Also, the steady-state values of per capita income and per capita consumption, which are obtained by normalizing with the population size, do also depend on both, the relative size of s_x and s_z and the fraction of infected individuals. Specifically, we have the following:

Corollary 1. *The steady-state values for per capita income and per capita consumption are given by*

$$y^{**} = A(k^{**})^{\alpha} \ ; \quad c^{**} = (1 - s_x)y^{**} . \tag{19}$$

in the disease-free steady state, and

$$y^* = \eta y^{**} \ ; \quad c^* = \left(\frac{1 - (s_x x^* + s_z z^*)}{1 - s_x} \right) \eta c^{**} . \tag{20}$$

in the pandemic steady state, where:

$$\eta = \left(\frac{s_x x^* + s_z z^*}{s_x} \right)^{\alpha/(1-\alpha)} x^* . \tag{21}$$

Proof. Since $y(t) = \dfrac{Y(t)}{N(t)} = (\dfrac{AK(t)^{\alpha}}{X(t)^{\alpha}})(\dfrac{X(t)}{N(t)})$ and $c(t) = [1 - (s_x x(t) + s_z z(t))]y(t)$, by substituting for each steady-state value of $x(t)$ and $z(t)$ we get the corresponding steady-state values of $y(t)$ and $c(t)$ in each equilibrium. Next, the parameter η is obtained by computing:

$$\eta = \frac{y^*}{y^{**}} = \left(\frac{k^*}{k^{**}} \right)^{\alpha} x^* = \left(\frac{s_x x^* + s_z z^*}{s_x} \right)^{\frac{\alpha}{(1-\alpha)}} x^* \tag{22}$$

It turns out that $\eta < 1$ in the pandemic steady state. This can be easily shown by, starting from its value at the disease-free steady state, checking that $\partial \eta / \partial z^* < 0$. By being a continuous function, the result follows. $\square$

Since $\eta < 1$, the pandemic equilibrium leads to a lower steady-state value for per capita income independently of the relative sizes of s_x and s_z. This is also true for the particular case in which $s_x = s_z$ since, in this case, $\eta = x^*$. However, per capita consumption could be greater in the pandemic steady state if $s_x > s_z$. This is so because, although $y^* < y^{**}$ always, the aggregate saving rate is lower in the pandemic steady state and this positive effect on per capita consumption could compensate the negative effect on per capita income. Of course, if $s_x \leqq s_z$, then c^* is unambiguously lower than c^{**}.

We next check the convergence to the pandemic steady state. The main result is summarized in the following proposition.
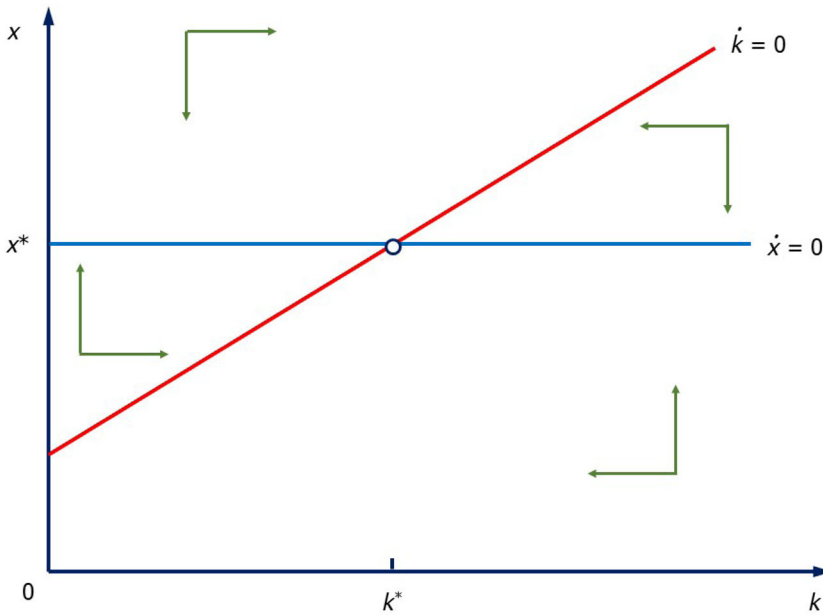
FIGURE 2 Linearized system of the SIS–Solow model [Colour figure can be viewed at wileyonlinelibrary.com]

Proposition 4. *Consider $\mathcal{R}_0 > 1$, then the linearized version of the two differential equations (4) and (15) around the pandemic steady-state solution (17) are given by the matrix system:*

$$\begin{bmatrix} \dot{x} \\ \dot{k} \end{bmatrix} = \begin{bmatrix} -b(1 - 1/\mathcal{R}_0) & 0 \\ \left(\dfrac{(s_x - s_z)(\delta + g)}{s_x - (s_x - s_z)z^*} + b(\mathcal{R}_0 - 1) \right)k^* & -(1 - \alpha)(\delta + g) \end{bmatrix} \begin{bmatrix} x - x^* \\ k - k^* \end{bmatrix}. \quad (23)$$

Hence, the resulting eigenvalues are two negative real roots so that the system is locally stable.

Proof. See the Appendix for the proof. □

Figure 2 illustrates the nature of the local stability of the pandemic steady state. The arrows in green show the motion of the variables. They point toward the locally stable steady state (k^*, x^*). To illustrate this approach, we can see the consequences of a change in the value of $\mathcal{R}_0$. In Figure 3, suppose that the economy begins at point E with $\mathcal{R}_0' = 1.50$ and then, there is a decrease in the recovery rate, a, that increases the basic reproductive number to $\mathcal{R}_0'' = 2.00$. The new steady-state equilibrium corresponds to the new pandemic solution with $1/\mathcal{R}_0''$ and a lower capital labor ratio k_F^*. As the figure shows, the increase in $\mathcal{R}_0$ causes a downward shift in both locus, $\dot{x} = 0$ and $\dot{k} = 0$.

The fall in a also causes a fall in the slope of the $\dot{k} = 0$ locus. In the path of convergence to the new steady state, the increase in $\mathcal{R}_0$ causes a fall in both, $x(t)$ and the growth rate in the population of susceptible individuals. As a result, $k(t)$ increases and the economy moves away from the initial equilibrium point, E. Once the steady-state value for the proportion of susceptible individuals is reached at point E', and $\dot{x} = 0$, the capital stock per noninfected individual begins to fall steadily until k_F^* is eventually reached at point F.
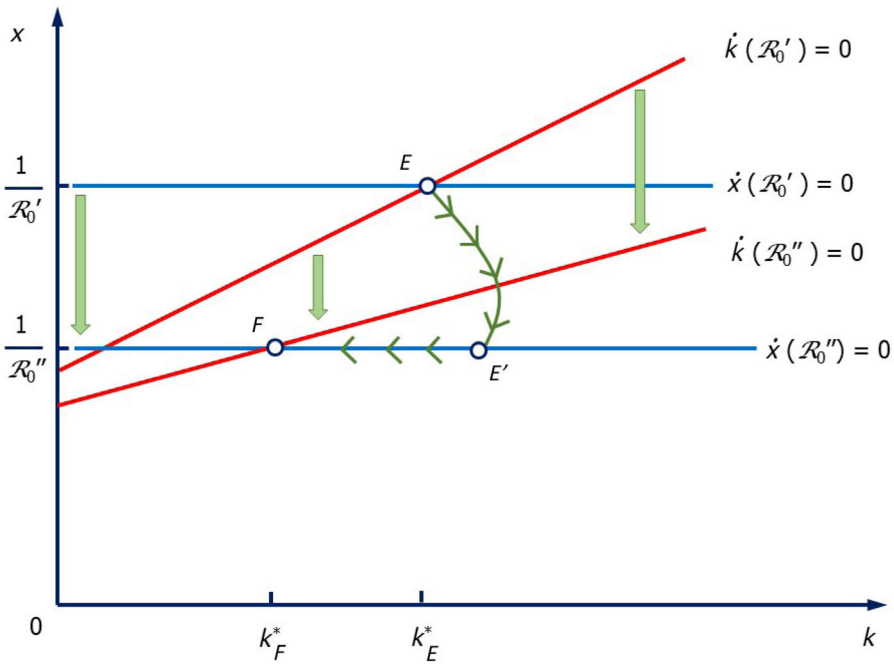
FIGURE 3 An increase of the basic reproductive number in the SIS–Solow model. In the initial equilibrium, $\mathcal{R}_0' = 1.50$, so that $x_E^* \approx 0.66$. In the final equilibrium, $\mathcal{R}_0'' = 2.00$, so that $x_F^* = 0.50$. The steady-state value of the capital stock per noninfected individual is lower in the final equilibrium $k_F^* < k_E^*$. [Colour figure can be viewed at wileyonlinelibrary.com]

To illustrate the time path followed by the fraction of infected individuals, z, and the other relevant economic variables k, y, and c along the adjustment path, we have obtained the exhibits in the left column of Figure 5. Observe that the path for k is hump-shaped because of the lag in k to adjust to the steady fall in the proportion of healthy individuals as the economy converges to the new pandemic steady state. For this simulation, the basic reproductive number in the initial steady state is $\mathcal{R}_0' \approx 1.50$, which corresponds to $b = 0.5$, $n = 0.03$, and $a = 0.3$. There is a decrease in the value of the rate of recovery from infection, $a = 0.22$, that leads to a basic reproductive number of $\mathcal{R}_0'' = 2.00$ in the final equilibrium. The values of the economic parameter used in the simulation are $s_x = 0.1$, $s_z = 0.08$, $\alpha = 1/3$, $\delta = 0.10$, $g = 0.01$, and $A = 10$.

5 | THE SIR PANDEMIC SOLOW MODEL

Next, we impose the SIR model into the Solow growth model, which we will refer to as the SIR pandemic Solow model. The differential equation describing capital stock accumulation is

$$\dot{K}(t) = [s_x - (s_x - s_z)z(t)]AK(t)^{\alpha}(X(t) + V(t))^{1-\alpha} - \delta K(t), \qquad (24)$$

where now the number of noninfected people includes the population of recovered individuals, $X(t) + V(t)$ and the aggregate saving rate is still given by Equation (13). This is so because, for simplicity, both susceptible and recovered individuals in the population have been assumed to

exhibit the same propensity to save, s_x. Therefore, to express Equation (24) per effective worker, we must divide both sides by $X(t) + V(t)$ and not by $N(t)$. Then, we have:

$$\dot{k}(t) = \frac{\dot{K}(t)}{X(t) + V(t)} - \frac{\dot{X}(t) + \dot{V}(t)}{X(t) + V(t)}k(t). \tag{25}$$

Notice that the term affecting $k(t)$ in the previous Equation (25) can be rewritten as:

$$\frac{\dfrac{\dot{X}(t) + \dot{V}(t)}{N(t)}}{\dfrac{X(t) + V(t)}{N(t)}} = \frac{\dot{x}(t) + \dot{v}(t) + g(x(t) + v(t))}{x(t) + v(t)} = \frac{-\dot{z}(t)}{1 - z(t)} + g. \tag{26}$$

Therefore, the growth rate of the capital stock per noninfected worker, $k(t)$, is driven by

$$\dot{k}(t) = [s_x - (s_x - s_z)z(t)]Ak(t)^\alpha - \left(\delta + g - \frac{\dot{z}(t)}{1 - z(t)}\right)k(t). \tag{27}$$

Using this equation, we obtain the following results.

Proposition 5. *If $\mathcal{R}_0 \leqq 1$, the disease-free steady state for the SIR pandemic Solow model is*

$$x^{**} = 1, \quad z^{**} = 0 \quad and \quad k^{**} = \left(\frac{s_x A}{\delta + g}\right)^{\frac{1}{(1-\alpha)}}. \tag{28}$$

Alternatively, if $\mathcal{R}_0 > 1$, the pandemic steady state is

$$x^* = \frac{1}{\mathcal{R}_0}, \quad z^* = \left(\frac{n}{a + n}\right)\left(1 - \frac{1}{\mathcal{R}_0}\right) \quad and \quad k^* = \left(\frac{s_x x^* + s_z z^*}{s_x}\right)^{\frac{1}{1-\alpha}} k^{**}. \tag{29}$$

Proof. The two equilibria follow from setting $\dot{x}(t) = 0$, $\dot{z}(t) = 0$, and $\dot{k}(t) = 0$ in Equations (6), (7), and (27), respectively. The value for k^{**} is then obtained by taking into account the same remark made in Proposition 3. □

The capital stock per noninfected worker ratio in each equilibrium is equal to those obtained in the previous section for the SIS pandemic Solow growth model. Thus, per capita output will be lower in the pandemic steady state for every possible value of s_x and s_z but the corresponding level of per capita consumption could be higher if $s_x > s_z$.

We turn next to examine the local stability of the SIR pandemic Solow model.

Proposition 6. *Consider $\mathcal{R}_0 > 1$, then the linearized versions of the three differential equations (6), (7), and (27) around the pandemic steady-state solution (29) are given by the matrix system*

$$\begin{bmatrix} \dot{x} \\ \dot{z} \\ \dot{k} \end{bmatrix} = \begin{bmatrix} -n\mathcal{R}_0 & -(a + n) & 0 \\ n(\mathcal{R}_0 - 1) & 0 & 0 \\ b\left(\dfrac{z^*}{1 - z^*}\right)k^* & -(s_x - s_z)A(k^*)^\alpha & -(1 - \alpha)(\delta + g^*) \end{bmatrix} \begin{bmatrix} x - x^* \\ z - z^* \\ k - k^* \end{bmatrix}. \tag{30}$$

If $n\theta_1 < b < n\theta_2$, with θ_1 and θ_2 as given in Proposition 2, the system has two imaginary roots with negative real part plus a third negative real root. In all other cases, the eigenvalues are three negative real roots. Hence, the system is locally stable and the convergence toward the steady state may be cyclical.

Proof. See the Appendix for the proof. □

As in the previous section, we carry out the same exercise of an increase in $\mathcal{R}_0$ as a result of a fall in the recovery rate, a. In this case, to depict graphically the convergence to the pandemic equilibrium we resort to a simulation that shows the cyclical path followed by the variables of interest. In the upper panel of Figure 4, we show the path followed by the proportion of susceptible individuals, $x(t)$, and the capital stock per non-infected worker, $k(t)$, until the new steady state is eventually reached. Similarly, in the lower panel of Figure 4, we show the path followed by the proportion of infected individuals, $x(t)$, and the capital stock per non-infected worker, $k(t)$, until the new steady state is eventually reached.

The initial equilibrium is given by $\mathcal{R}'_0 \approx 1.50$ (corresponding to $a = 0.30$, $b = 0.50$, and $n = 0.03$) , $x^*_E \approx 0.67$, $z^*_E \approx 0.030$, and $k^*_E \approx 27.16$. The final equilibrium is given by $\mathcal{R}''_0 = 2.00$ (corresponding to $a = 0.22$, $b = 0.50$, and $n = 0.03$), $x^*_F = 0.50$, $z^*_F = 0.06$, and $k^*_F \approx 26.92$. The remaining parameters used in the simulation has been $s_x = 0.1$, $s_z = 0.03$, $\alpha = 1/3$, $\delta = 0.10$, $g = 0.01$, and $A = 10$. As shown, convergence takes place cyclically.
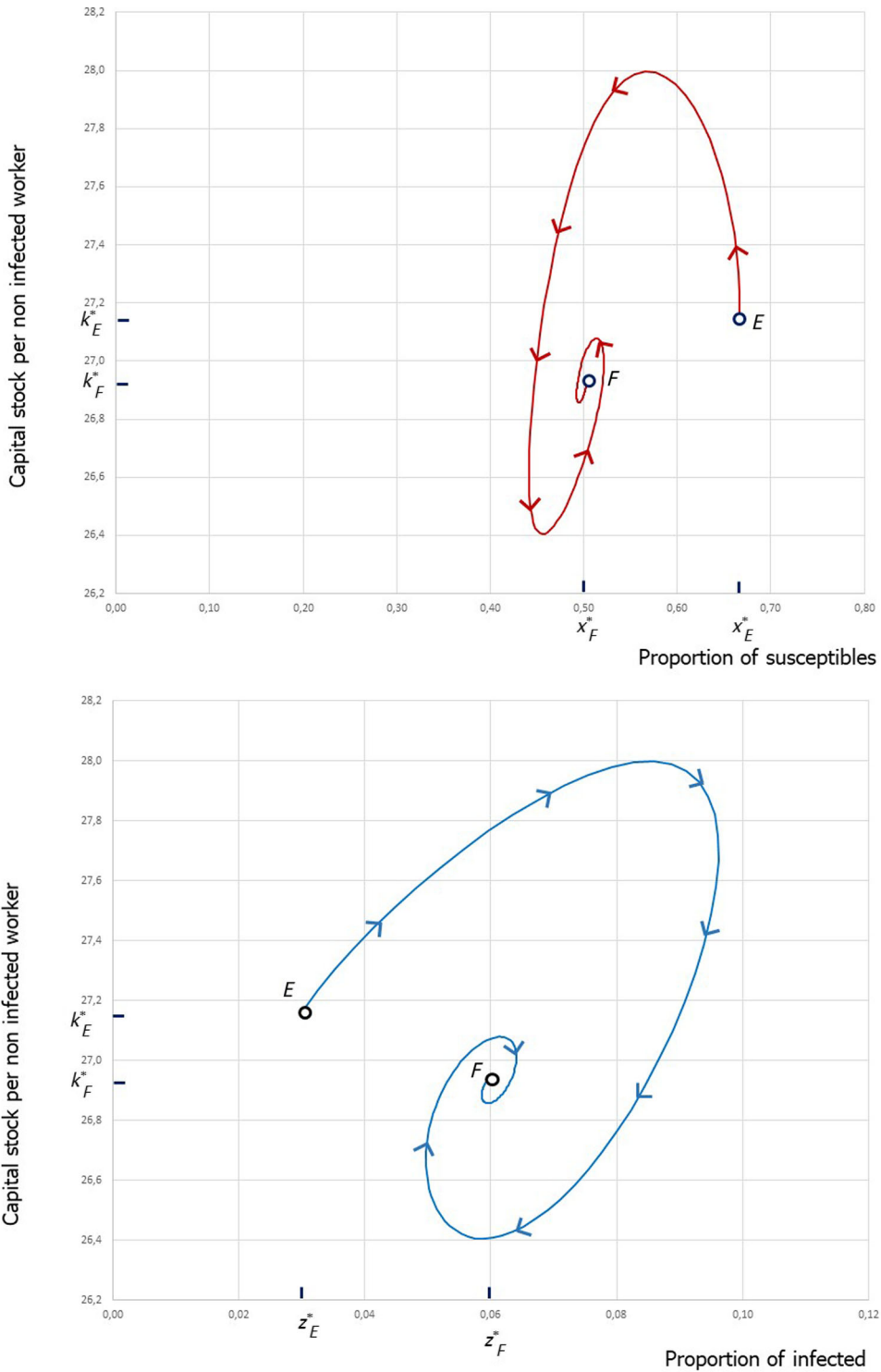
As in the case of the pandemic SIS–Solow model, we compute the time path followed by z and the economic relevant variables k, y, and c, to illustrate their dynamics. They are depicted in the right column of Figure 5. Given the previous values for the parameters describing how the disease spreads, the convergence to the new pandemic steady state is cyclical.

6 | CONCLUSIONS

In our review of the standard models of disease, we have shown that when population grows at some positive rate, and by using the standard incidence definition, the solutions to the long-run proportion of susceptible individuals are given by the inverse of the basic reproductive number, $\mathcal{R}_0$, in the pandemic equilibrium, and by one in the disease-free alternative. This is analogous to the constant population case with the only change of its specific definition, namely, as whether or not the birth rate is added to the recovering rate in the denominator. The convergence to the long-run values of the proportions of individuals is uniform for the SIS case and may be cyclical for the SIR case. But in both cases, once the population of susceptible individuals achieve the herd immunity thresholds, the disease dies out with the proportion of infected individuals not growing again above the maximum value achieved previously.

When including either of the previous disease models into a Solow growth model with an aggregate saving rate that depends upon the fraction of infected individuals, we find that the capital stock per noninfected individual in the pandemic steady state could be greater than the corresponding one for the disease-free equilibrium if s_z is higher than s_x. However, per capita income is always lower in the pandemic equilibrium independently of the relative sizes of s_x and s_z. Finally, per capita consumption could be higher in the pandemic equilibrium if $s_x > s_z$.

Following Goenka and Liu (2012), there are several extensions regarding to this approach about the impact of diseases in economic growth. One of them is to introduce a fatality rate that increases the death rate as a result of the disease. Intuitively, by reducing the value of the vegetative growth,

FIGURE 4 An increase of the basic reproductive number in the Pandemic SIR–Solow model. Initial equilibrium, $\mathcal{R}'_0 = 1.50$, with $x^*_E \approx 0.66$ and $k^*_E = 27.16$. Final equilibrium, $\mathcal{R}''_0 = 2.00$, with $x^*_F = 0.50$ and $k^*_F = 26.92$. The values of the economic parameters used in the simulation are $s_x = 0.1$, $s_z = 0.08$, $\alpha = 1/3$, $\delta = 0.10$, $g = 0.01$, and $A = 10$. [Colour figure can be viewed at wileyonlinelibrary.com]
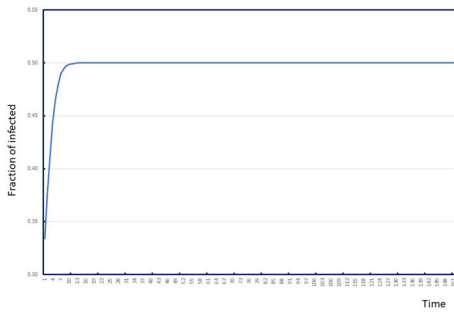
(a) Fraction of infected population.
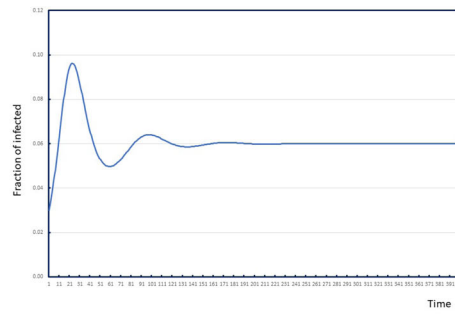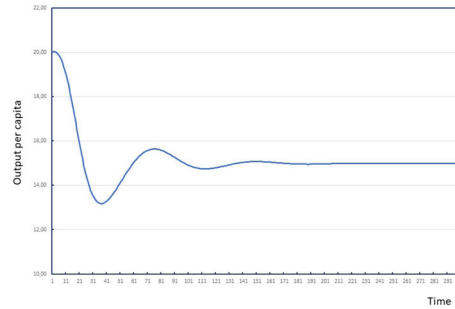
(b) Fraction of infected population.
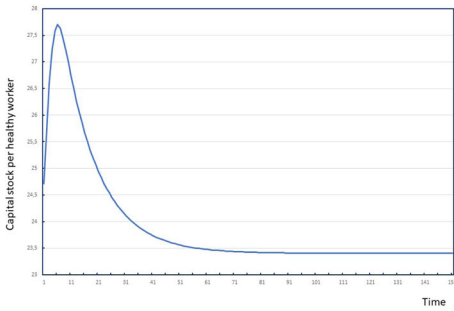
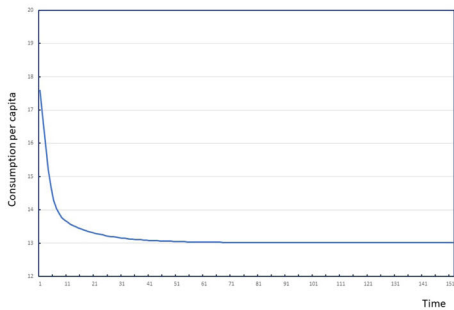(c) Capital per noninfected individual.
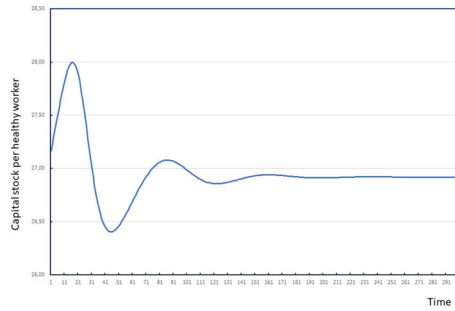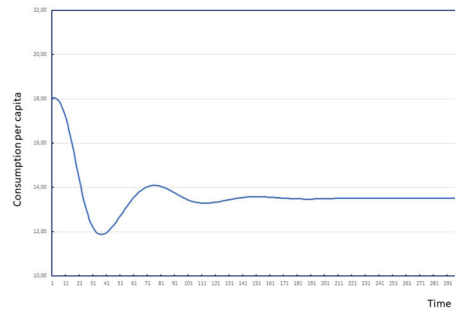
(d) Capital per noninfected individual.
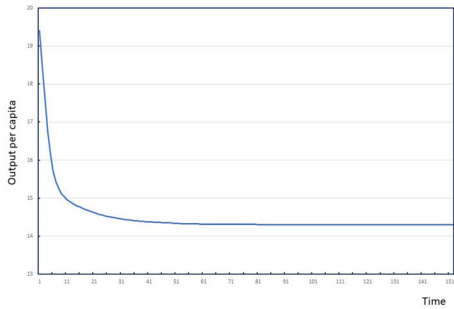
(e) Output per capita.

(f) Output per capita.

(g) Consumption per capita.

(h) Consumption per capita.

FIGURE 5   This panel depicts the adjustment path followed for the relevant variables after a decrease of parameter a in the pandemic SIS–Solow model (left column) and in the pandemic SIR–Solow model (right column). The parameters used in the simulations are those used for Figure 4. [Colour figure can be viewed at wileyonlinelibrary.com]

the fraction of infected individuals in the pandemic steady state will affect not only the level of output per capita but also its rate of growth. The recent paper of Goenka et al. (2021) is an outstanding example of the issues involved.

Another channel through which the epidemic has an influence in the long-run level of output per capita is through the total factor productivity term, A. A simple approach, along the lines of the present analysis, is to assume that the rate of growth of A depends on the fraction of population involved in research, following the seminal work of Uzawa (1965) and Lucas (1988). Again, only healthy individuals could work on the sector.[7] Our preliminary results show that, in the absence of any effect on the aggregate saving rate of the fraction of ill individuals in the final steady state, the capital stock per efficiency unit of healthy worker is the same regardless of the steady state. Of course, output per capita and consumption per capita are both lower in the pandemic steady state as a result of the higher fraction of ill individuals in that state. The results are available from the authors upon request.

ACKNOWLEDGMENTS

REFERENCES

Acemoglu, D. (2022). Confronting the challenges of post-COVID world. *Prospects of the Global Economy after COVID-19* (pp. 7–32). CEP and KIFs. https://voxeu.org/article/prospects-global-economy-after-covid-19

Acemoglu, D., Chernozhukov, V., Werning, I., & Whinston, M. D. (2020). *Optimal targeted lockdowns in a multi-group SIR model*. Working Paper 27102. http://www.nber.org/papers/w27102

Ahmetolan, S., Bilge, A. H., Demirci, A., Peker-Dobie, A., & Ergonul, O. (2020). What can we estimate from fatality and infectious case data using the susceptible-infected-removed (SIR) model? A case study of COVID-19 pandemic. *Frontiers in Medicine*, 7. http://doi.org/10.3389/fmed.2020.556366

Allen, L.J.S. (2008). Mathermatical Epidemiology. Springer-Verlag. Volume 145. chapter *An Introduction to Stochastic Epidemic Models*. pp. 81–130.

Avery, C., Bossert, W., Clark, A., Ellison, G., & Ellison, S. F. (2020). An economist's guide to epidemiology models of infectious disease. *Journal of Economic Perspectives*, 34(4), 79–104.

dos Santos, I., Almeida, G., & de Moura, F. (2021). Adaptive SIR model for propagation of SARS-CoV-2 in Brazil. *Physica A: Statistical Mechanics and Its Applications*, 569, 125773.

Eichenbaum, M. S., Rebelo, S., & Trabandt, M. (2020). *The macroeconomics of epidemics*. Working Paper 26882. http://www.nber.org/papers/w27128

Fernandez-Villaverde, J., & Jones, C. I. (2020). *Estimating and simulating a SIRD model of COVID-19 for many countries, states, and cities*. Working Paper 27128. http://www.nber.org/papers/w26882

Gersowitz, M., & Hammer, J. S. (2004). The economical control of infectious diseases. *Economic Journal*, 114(492), 1–27.

Goenka, A., & Liu, L. (2012). Infectious diseases and endogenous fluctuations. *Economic Theory*, 50(1), 125–149.

Goenka, A., & Liu, L. (2020). Infectious diseases, human capital and economic growth. *Economic Theory*, 70, 1–47.

---

[7] Alternatively and inspired by the comments of an anonymous referee about the possibility of telecommuting, one might consider the direction of technological change. Acemoglu (2022) points out that COVID-19 pandemic has accelerated automation as natural result of the increased demand for social distancing. The impact on technological progress of a pandemic surely will imply the development of technologies that do not require, at least for white-collar workers, to be present at the workplace. This is an intensification of the automation trends already present in the investment plans of most firms.

Goenka, A., Liu, L., & Nguyen, M. H. (2014). Infectious diseases and economic growth. *Journal of Mathematical Economics*, *50*, 34–53.

Goenka, A., Liu, L., & Nguyen, M. H. (2021). SIR economic epidemiological models with disease induced mortality. *Journal of Mathematical Economics*, *93*, 1–16.

Hethcote, H. W. (2008). *The basic epidemiology models: Models, expressions for $\mathcal{R}_0$, parameter estimation, and applications* (pp. 1–61). World Scientific Publishing.

Jones, C. I., & Vollrath, D. (2013). *Introduction to economic growth* (2nd ed.). W.W. Norton and Company.

Lucas, R. E. J. (1988). On the mechanics of economic development planning. *Journal of Monetary Economics*, *22*(1), 3–42.

Martcheva, M. (2015). *An introduction to mathematical epidemiology* (Vol. 61). Springer.

Moein, S., Nickaeen, N., Roointan, A., Borhani, N., Heidary, Z., Javanmard, S. H., Ghaisari, J., & Gheisari, Y. (2021). Inefficiency of SIR models in forecasting COVID-19 epidemic: A case study of Isfahan. *Scientific Reports*, *11*.

Roda, W. C., Varughese, M. B., Han, D., & Li, M. Y. (2020). Why is it difficult to accurately predict the COVID-19 epidemic? *Infectious Disease Modelling*, *5*, 271–281.

Shabbir, G., Khan, H., & Sadiq, M. (2010). A note on exact solution of SIR and SIS epidemic models. arXiv e-prints arXiv:1012.5035.

Sydsaeter, K., Hammond, P., Seierstad, A., & Strom, A. (2008). *Further Mathematics for Economic Analysis*. 2nd ed., Pearson Education.

Uzawa, H. (1965). Optimal technical change in an aggregative model of economic growth. *International Economic Review*, *6*(1), 18–31.

SUPPORTING INFORMATION

Additional supporting information can be found online in the Supporting Information section at the end of this article.